HIGH-RESOLUTION OBSERVATION AND DETAILED PHOTOMETRY OF A GREAT Hα TWO-RIBBON FLARE*

T. KITAHARA and H. KUROKAWA

Kwasan & Hida Observatory, Kyoto University, Kamitakara, Gifu 506–13, Japan

(Received 15 August, 1989)

Abstract. A great Hα two-ribbon flare of 12 October, 1981 was observed with the Domeless Solar Telescope at the Hida Observatory and its detailed photometry was made with a two dimensional microdensitometer. The principal results are as follows: (1) The impulsive phase of the flare started with the progressive brightenings of flare points forming the front lines of the Hα two ribbons at both sides of the magnetic neutral line. These are followed by the explosive expansion of Hα two ribbons at the main impulsive phase. (2) Three typical shapes of Hα light curves were found. The type 1 light curve is characterized by the primary impulsive rise and rapid fall of intensity. The light curve of type 3 has no impulsive component but has a very gradual maximum. The type 2 profile attains the main gradual maximum with a few small impulsive peaks. These different types of light curves are made by different heating mechanisms, those are electron precipitation, heat conduction and soft X-ray radiation respectively. (3) The light curve of total intensity, which was made by integrating Hα – 1.0 Å intensities of the whole main Hα flare region, shows a primary impulsive peak and a later gradual maximum. The former peak coincides in time with that of the hard X-ray emission. The latter maximum is well correlated with the soft X-ray maximum. (4) The brightest flare points with time profiles of type 1 are closely related to the impulsive hard X-ray emissions of highest energy.

1. Introduction

It has been widely believed that the time profile of Hα flare intensity variation is similar to that of soft X-ray flux through all stages of flare development, as described in the textbook of Švestka (1976) and the review of Kahler *et al.* (1980). The impulsive brightening features of Hα intensities could not be correctly studied with the conventional Hα flare patrol films of low resolution from which Kahler *et al.* (1980) and Švestka (1976) derived their Hα light curves.

Recent observations of high-spatial and temporal resolution have revealed a new important aspect of Hα light curves at the impulsive phases of flares; Kurokawa *et al.* (1986) and Kurokawa (1986) demonstrated impulsive and successive brightenings of Hα flare points at the impulsive phases of flares and showed that these spiky Hα brightenings are closely correlated in time to the impulsive fluctuations of hard X-ray and microwave emissions. Since these Hα flare points correspond to the footpoints of the flare loops, the detailed study of their successive brightening features will be an effective clue to examine the energy release and energy transport mechanisms in flare loops.

The great two-ribbon flare of 12 October, 1981, whose importance is 3B in Hα and X12 in soft X-ray, was fully recorded with the Domeless Solar Telescope at the Hida Observatory. A lot of high-resolution images of the flare were taken alternatively in the wavelengths of Hα center and Hα – 1.0 Å with Zeiss Hα Lyot filter through every stage of the flare. Several pictures were also obtained in Hα – 5.0 Å and Hα – 13.0 Å around

* Contributions from he Kwasan and Hida Observatories, Kyoto University, No. 297.

Solar Physics **125:** 321–332, 1990.

the maximum phase of the flare. A full description of the flare development will be given in a separate paper.

We measured 147 images of Hα – 1.0 Å with the two-dimensional microdensitometer at the Institute of Astrophysics, Kyoto University and determined the light curves in Hα – 1.0 Å for 800 points in the main Hα emitting region of the flare. It is the first attempt to study such a great amount of light curves of individual flare points over such a large two-ribbon-flare region. Examining these data, we study evolutional characteristics of the Hα two-ribbon flare referring to the evolution of X-ray emissions observed by ISEE-3 and GOES satellites.

2. Rapid Development of Hα Emitting Region

Selected pictures in Hα – 1.0 Å show the rapid development of the Hα emitting region during the impulsive phase of the flare in Figure 1. This flare is a very big event and Hα brightenings occurred over the extended area. In this paper, however, we focus our studies on the main flare region which developed along the neutral line between the main bipolar sunspots *A* and *B* (Figure 2). We find two stages of impulsive growth of the Hα emitting region; (1) successive brightenings of flare points along the magnetic neutral line, and (2) rapid expansion of Hα two ribbons (explosive phase).

At the first stage (Figures 1 (a)–(d)), many flare points successively brighten to form the front lines of so-called Hα two-ribbons at the both sides of the magnetic neutral line. The paths and directions of the progressive brightenings are shown with arrows in Figure 2, where the outer boundaries of the sunspot umbrae and penumbrae are indicated by full and dotted lines, respectively. Notice the progressive brightenings of flare points along the outer boundary of the penumbra of sunspot *A*. The light curves of the flare points marked in Figure 2 are obtained by the procedure to be described in the next section and given in Figure 3. We can see successive rising-ups of the light curves for one flare point after another. We can measure the propagation speeds of the progressive brightenings along the line 1–2–3–4–5 indicated in Figure 2. The measured mean speeds are not uniform, but are 97 km s^{-1} for 1–2–3 propagation and 267 km s^{-1} for 3–4–5 propagation, respectively. Vorpahl (1972) suggested a magnetosonic wave as the propagating mechanism triggering sequential loop activations and estimated its velocity range between 330 and 450 km s^{-1} using an electron flare density of 2×10^{11} cm^{-3}, the magnetic field strength between 50 and 80 and the temperature of the ambient corona of 1.5×10^6 K. The former speed 97 km s^{-1} measured above is much smaller than the range estimated by Vorpahl (1972), while the latter speed is 267 km s^{-1} near the range of magnetosonic velocity. Kawaguchi *et al.* (1982) also found a wide variety of speeds of Hα progressive brightenings for a subflare.

The expansion (the second stage development) of Hα emission strands started around 06:25 UT. The front lines of Hα two ribbons moved toward the direction opposite to each other (Figure 1). The direction of the expansion is shown by the line a–b–c–d for one of Hα-ribbon in Figure 2. The time profiles of the points a–b–c–d in Figure 3 successively rise up with strong impulsiveness. We measured the expanding speed

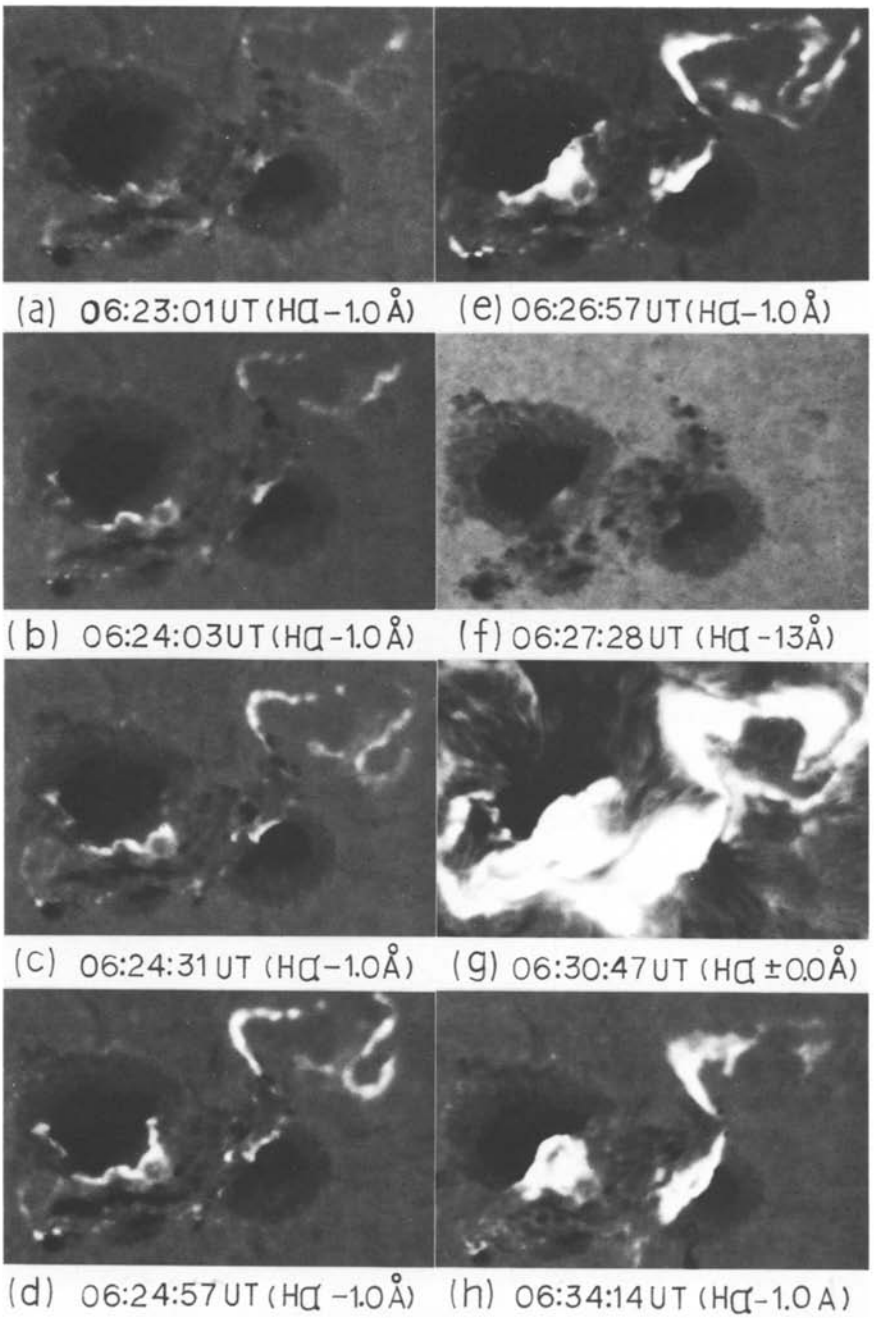

Fig. 1. Selected Hα pictures of the 12 October, 1981 two-ribbon flare. The central wavelength of the pictures (a)–(e) and (h) is Hα – 1.0 Å, and those of (f) and (h) are Hα – 13 Å and Hα center, respectively.

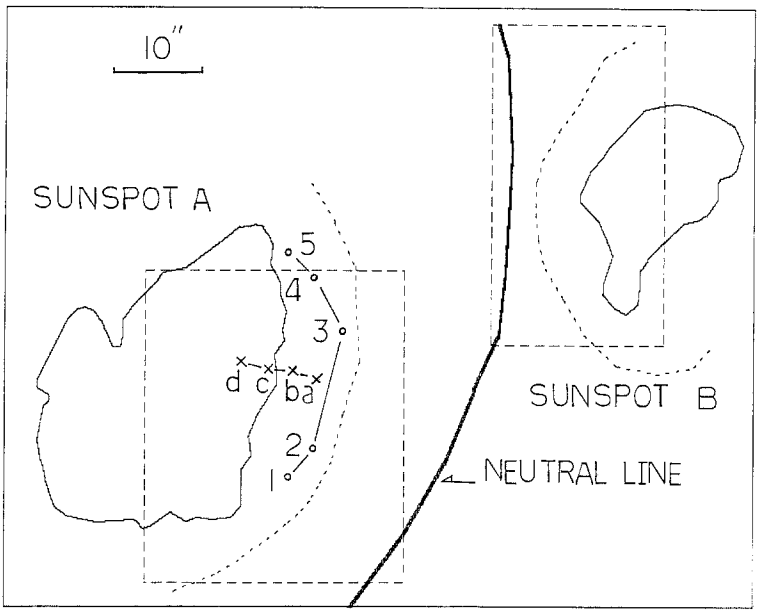

Fig. 2. A sketch of the flare region. The outer boundaries of the sunspot umbrae and penumbrae are indicated by full and dotted lines, respectively. Broken lines show the areas scanned by the two-dimensional microdensitometer. The path of the progressive brightenings at the first stage of the impulsive phase is shown by the line 1–2–3–4–5 in sunspot *A*. The line a–b–c–d shows the direction of the Hα-ribbon expansion at the second stage of the impulsive phase.

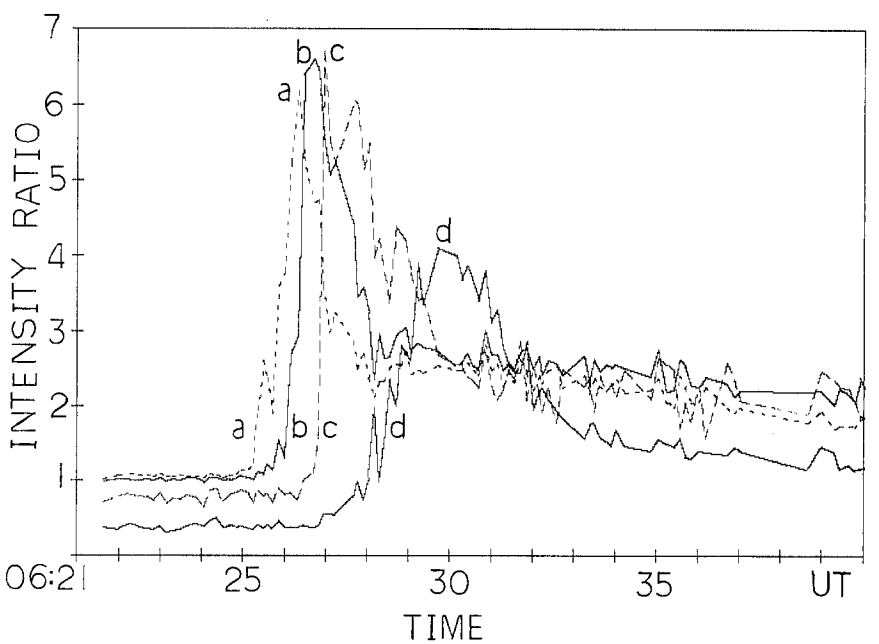

Fig. 3. Hα light curves of the points a, b, c, and d shown by crosses in Figure 2. The ordinate gives intensity ratios or intensities of flare points relative to the mean intensity of a quiet region near the flare. The abrupt and successive rising-up of light curves corresponds to the rapid expansion of the Hα ribbon.

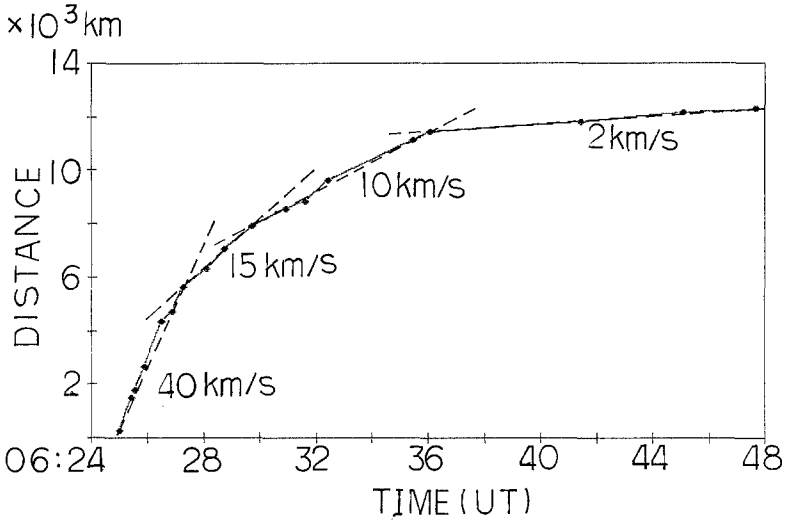

Fig. 4. The time variation of measured expanding speeds of the Hα ribbon in the sunspot *A* region. The ordinate shows the distance between the front line of the Hα ribbon and a fixed point.

perpendicular to the long axis of each Hα ribbon on the contour maps of Hα images. The time variation of measured expanding speeds is shown for the spot *A* in Figure 4. Notice the very large speed for the initial expansion of Hα two ribbons or 40 km s^{-1} and the abrupt slow-down at 06:27 UT when the Hα front line invaded umbrae (Figure 1). The speed of 40 km s^{-1} is much larger than the one reported by the text book of Švestka (1976) but may be typical of the initial expansions of big two-ribbon flares.

3. Three Typical Shapes of Hα Light Curves

One hundred and forty seven pictures of Hα – 1.0 Å taken from 06:21:38 UT to 06:47:40 UT were measured by the two-dimensional microdensitometer. The scanned area is indicated in Figure 2 by broken lines. We randomly selected 450 and 308 pixels in the scanned region of the preceding (sunspot *A* region) and following (sunspot *B* region) magnetic polarity, respectively, and constructed their light curves. The size of each pixel is 1.5″ × 1.5″.

Examining 758 light curves, we found the three typical shapes, which are given in Figure 5. Type 1 light curve is characterized by an abrupt increase and rapid fall of intensity just like an impulsive spike of hard X-ray emission. The peak intensity I_p of a typical type 1 profile is much larger than those of other types. Almost all light curves whose peak intensities are larger than $4.0 I_0$ are identified with type 1, where I_0 is the mean intensity of a quiet region near the flare. The impulsive peak of the type 1 is attained in a very short time or only 10 through 30 s. The type 1 profile has a second gradual maximum. The time difference between the first impulsive and the second gradual peaks ranges from 2 to 3 min for 93% of type 1 profiles.

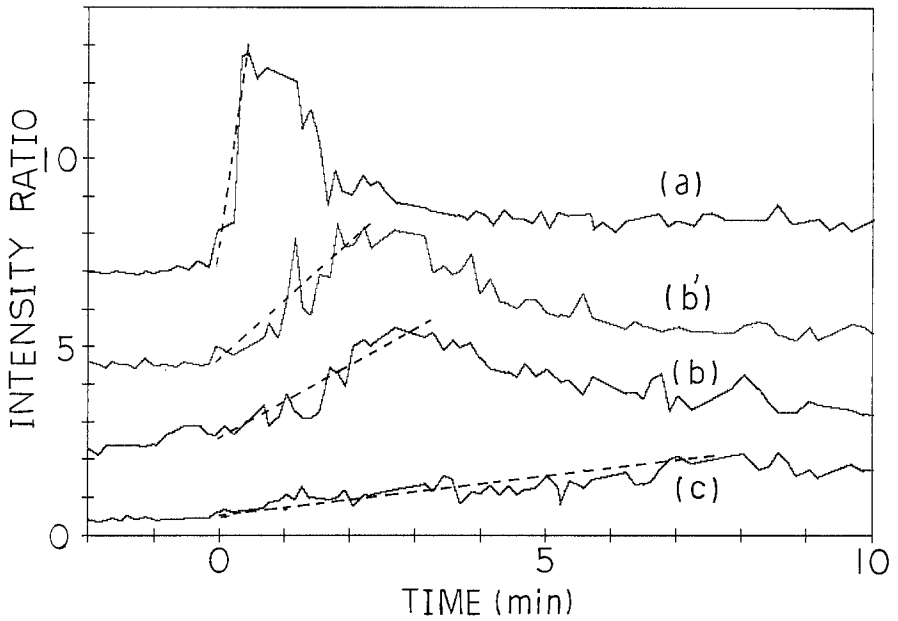

Fig. 5. The three typical shapes of Hα light curves. The type 1 profile (a) is characterized by a main impulsive peak and the second gradual maximum. The type 2 profile (b) is characterized by a main gradual maximum. Some type 2 profiles (b′) have minor impulsive spikes. The type 3 profile is characterized by a very slow rising slope or has a gradual hill shown by (c). The intensity ratio of the ordinate means the intensity of Hα flare point divided by the mean intensity of a quiet region near the flare. Since the origins of the ordinate are increased by 6, 4, and 2 for the light curves (a), (b′), and (b), respectively, the real intensity ratios are obtained by subtracting 6, 4, and 2 from those in the figure for (a), (b′), and (b), respectively. The mean inclination of the rising-slope of each light curve is shown by broken lines.

A typical profile of the type 2 is given in Figure 5(b). It attains its gradual main maximum in 2 or 3 min. This main maximum of the type 2 profile is very similar in shape to the second gradual maximum of the type 1 profile. On its rising slope it often has a few small impulsive peaks. These impulsive peaks of the type 2 profile seem to have failed to grow as large as that of the type 1 because of a deficiency of a proper heating agent. There are some light curves whose shapes are intermediate between the type 1 and type 2. The profile whose gradual main maximum is larger than the foregoing impulsive peaks is classified as type 2. Such an example is given in Figure 5(b′).

The light curve of the type 3 is distinguished by a very slow increase and has a gradual hill without any impulsive peak. A typical rising time from the start to the maximum of the type 3 light curve ranges from 5 to 7 min. The peak intensity ratio I_p/I_0 of the type 3 profile is less than 2.5 and much lower than that of the type 1.

Figure 6 shows the distribution of the three types of light curves in the diagram defined by two parameters dI/dt and I_p/I_0, where dI/dt is the mean inclination of the primary rising-slope of each light curve as shown by broken lines in Figure 5. The group of the type 1 light curves is characterized by large dI/dt and large I_p/I_0, and the type 3 by small dI/dt and small I_p/I_0.

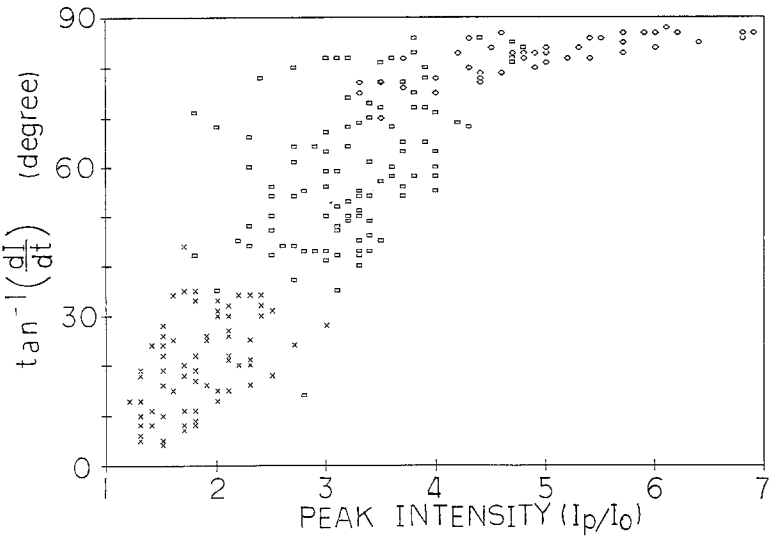

Fig. 6. The distribution of the three types of light curves in the diagram defined by dI/dt and I_p/I_0. A parameter dI/dt is the mean inclination as shown in Figure 5. I_p/I_0 is the ratio between the peak intensity of a light curve I_p and the mean intensity I_0 of a quiet region near the flare.

The group of type 2 is located between the type 1 and the type 3. Notice that the points of $I_p/I_0 > 4.0$ always have the largest values of dI/dt and belong to the type 1 class. This means that the brightest flare points are heated by a specially impulsive heating mechanism.

The spatial distribution of the three types of light curves is shown in Figure 7 where the points of the type 1, type 2, and type 3 are indicated, respectively, by circles, squares and crosses and the umbra and penumbra of the sunspot A are encircled by full and dotted lines, respectively. Most of flare points rising up during the first stage of the flare development are difficult to be definitely classified because of their low peak intensities and indistinct shapes of time profiles. The points of the typical type 1 light curves are mainly located over the sunspot penumbrae where the progressive brightenings of flare points and the initial explosive expansion of Hα two ribbons occurred. Most of the type 2 points are found inside the sunspot umbrae and around the boundary between penumbrae and umbrae. The type 3 points are mainly located at the outermost part of the Hα flare region. The spatial distributions of the three types reflect the evolutionary characteristics of the Hα flare development.

The type 1 points were made at the impulsive phase of the flare. The majority of flare points or kernel points, which successively brightened at the impulsive phase, show a type 1 profile. Especially, the brightest type 1 points are concentrated in the main impulsive phase (explosive phase) between 06:26 UT and 06:27 UT when hard X-ray emissions (70–168 keV) observed by ISEE-3 also attain their main impulsive peak (Figure 8). The type 2 points are most abundant in the sunspot umbra between 06:28 UT and 06:32 UT. The number of the type 3 points increased even after the hard

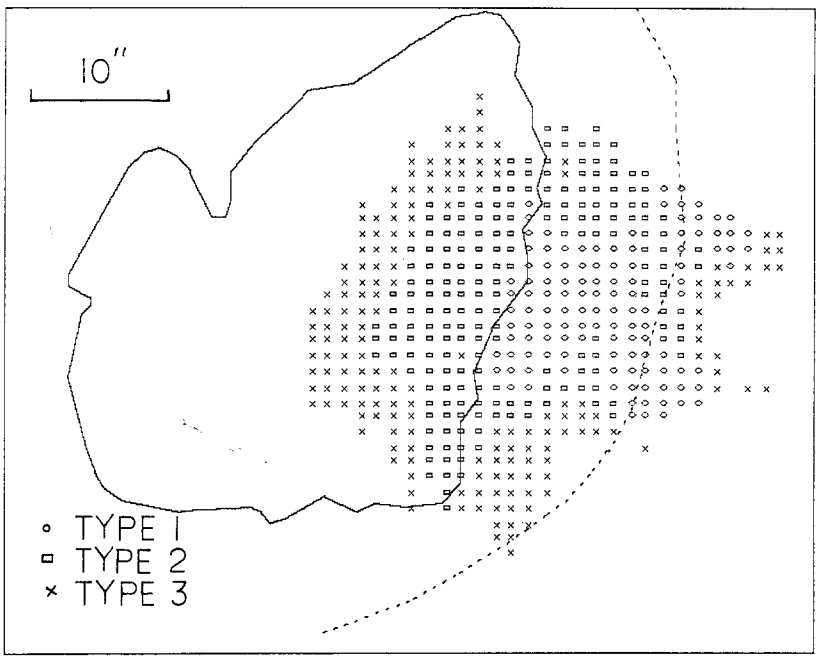

Fig. 7. The spatial distribution of the three types of light curves. The points of type 1, type 2, and type 3 are indicated by circles, squares and crosses, respectively. The umbra and penumbra of sunspot *A* are encircled by full and dotted lines, respectively.

X-ray maximum and reached its maximum around 06:34 UT when soft X-ray flux showed its gradual maximum according to GOES-3 observation (Figure 8).

It is likely that the three types of light curves recognized above are caused by different heating mechanisms. The energy released in the corona is transported to the chromosphere mainly by two agents, nonthermal electron beams and heat conduction (Švestka, 1976). Brown (1973) studied a chromospheric flare model heated by beams of nonthermal electrons, and many investigators now believe the existence of nonthermal electrons in the impulsive phase chromosphere (Brown, 1986). In fact, Kurokawa, Takakura, and Ohki (1988) showed that electron beam precipitation is the principal heating mechanism of the flare chromosphere at the early impulsive phase of the 23 March, 1982 flare by referring to the close temporal correlation between Hα and hard X-ray emissions. We may hereby assume that the impulsive peak of the type 1 light curves is made by nonthermal electron beams, because almost all the type 1 profiles attain their impulsive peaks at the impulsive phase of this flare (Figure 7). The gradual peaks which were found in the second maximum of the type 1 and the main maximum of the type 2 may be produced by another heating agent or heat conduction. The type 3 profile must reflect a much slower energy release and/or heating mechanism. Since it has no spiky conponent which may be produced by the impulsive particle-precipitation, the type 3 emission is considered to be excited by heat conduction or soft X-ray

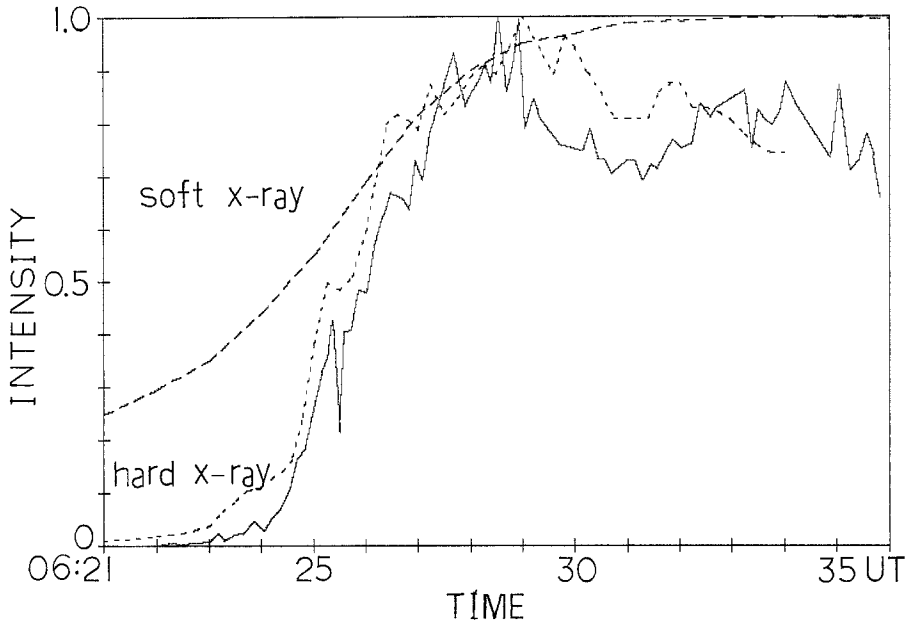

Fig. 8a. The light curves of the total Hα − 1.0 Å intensity (full line) compared with the time profiles of hard X-rays of 20–37 keV and soft X-rays of 0.5–4.0 Å. The total Hα − 1.0 Å intensity was obtained by integrating all Hα − 1.0 Å intensities larger than 1.5 I_0 where I_0 is the mean intensity of the nonflare region. The time profiles of the hard and soft X-ray emissions are given by the dotted line and the broken line, respectively. The maximum intensity of each emission is normalized to be unity.

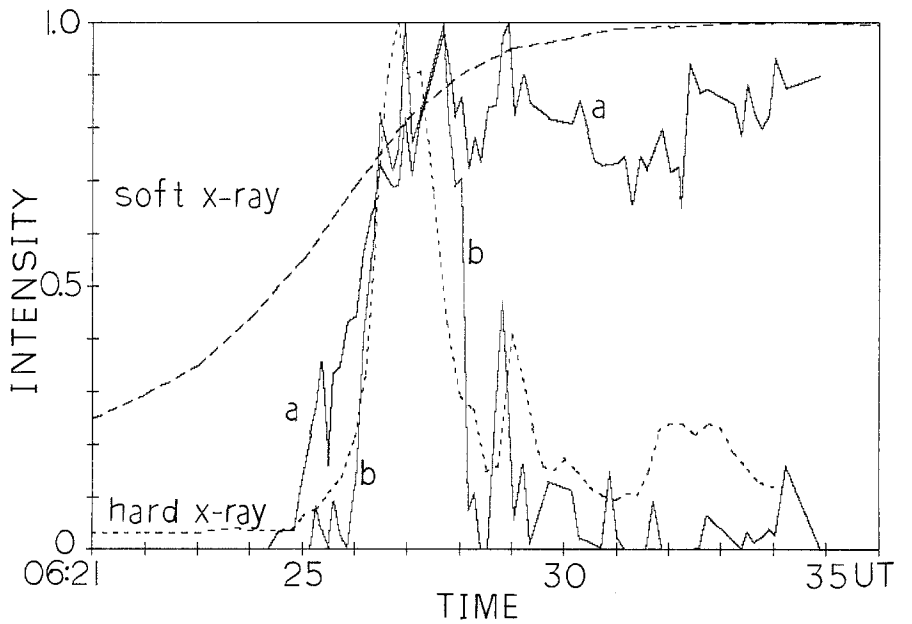

Fig. 8b. Same as Figure 8a, but the hard X-ray range is of 70–168 keV and the total Hα − 1.0 Å intensities (a) and (b) are obtained for all the pixels of $1.5 < I/I_0 < 2.5$ and $I/I_0 > 4.0$, respectively.

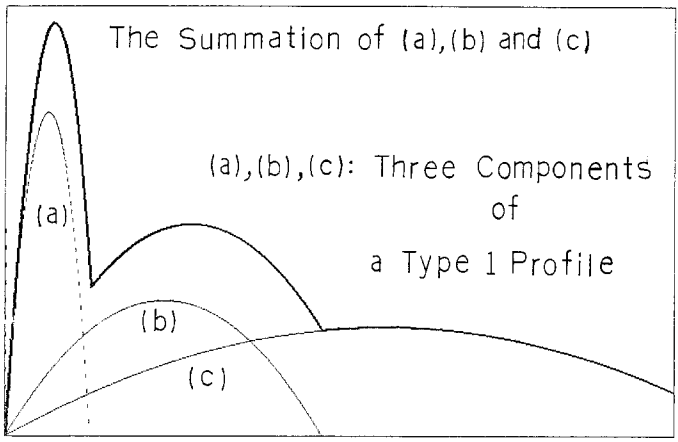

Fig. 9. Schematic curve of the typical type 1 profile decomposed into three components, which are (a) the first impulsive component due to fast electron beams, (b) the second maximum due to the fast heat conduction, and (c) the late gradual component due to the slow thermal flow or soft X-ray radiation.

radiation. The temporal coincidence between the number of the type 3 points and soft X-ray flux is consistent with this conclusion.

Type 1 profile seems to consist of three parts; the first impulsive component which characterizes the type 1, the second maximum as in the type 2 and late gradual component as in the type 3. Figure 9 demonstrates a type 1 profile decomposed into the three components. It may be inferred, therefore, that the type 1 point is firstly excited by fast electron beams, secondly by the fast heat conduction front and thirdly by the slow thermal flow or soft X-ray radiation.

4. Temporal Correlation between Hα and X-ray Emission

It was implied in the previous sections, that the successive brightenings of Hα flare points and explosive expansion of Hα two-ribbons are closely correlated to the impulsive increase of the hard X-ray emissions at the impulsive phase of the flare and that the gradual increases of Hα light curves at the later phase are similar to those of the soft X-ray emissions. In this section, we will study these correlations in more detail.

Since the X-ray flux observed by ISEE-3 (hard X-ray) and GOES-3 (soft X-ray) are integrated over the whole flare region, we also calculated the total Hα − 1.0 Å intensity by integrating the Hα − 1.0 Å intensities of all measured points over the whole main Hα flare region indicated in Figure 2.

The obtained light curves of the total Hα − 1.0 Å intensity were compared with the time profiles of hard X-rays of 20–37 keV and 70–168 keV and soft X-rays of 0.5–4.0 Å in Figures 8(a) and 8(b). The hard X-ray and soft X-ray data were supplied by Dr Kane and Dr Cowley, respectively. The total Hα − 1.0 Å intensity of Figure 8(a) was obtained by integrating over all pixels with Hα − 1.0 Å intensity I larger than $1.5I_0$ where I_0 is the mean intensity of the nonflare region, and $1.5I_0$ is the minimum flare intensity safely

exceeding the observational error bar. The light curve for $I/I_0 > 1.5$ shows two outstanding maxima (Figure 8(a)). The first maximum is well correlated in time to that of 20–37 keV hard X-rays within the temporal resolution of the Hα observation. This is the first that clearly demonstrated the good temporal correlation between hard X-ray flux and the Hα total intensity integrated over the whole Hα flare region, though we have already showed the good correspondence between the successive brightenings of flare points or kernels and impulsive spikes of hard X-ray emissions (Kurokawa *et al.*, 1986; Kurokawa, 1986; Kurokawa, Takakura, and Ohki, 1988). The second gradual maximum is well correlated to that of the soft X-rays. This correspondence has already been stressed in the conventional text books (Priest, 1981; Kahler *et al.*, 1980; Švestka, 1976).

The Hα total intensities of the two light curves of Figure 8(b) were obtained for all the pixels of $1.5 < I/I_0 < 2.5$ and $I/I_0 > 4.0$, respectively. The light curve for the brightest Hα emitting region of $I/I_0 > 4.0$ only shows an impulsive peak around 06:27 UT well-correlated with that of hard X-ray of the highest energy range or 70–168 keV. As shown in Section 3, almost all the points of $I/I_0 > 4.0$ show the type 1 light curves and the brightest type 1 points are concentrated in the main impulsive phase when hard X-ray emissions (70–168 keV) attain their main impulsive peak. This means that the strongest chromospheric heating occurred nearly simultaneously when the highest energy electrons were accelerated in the flare loops if the thick-target model of hard X-ray is assumed. Then it is likely that the footpoints of most energetic flare loops, where impulsive hard X-ray emissions of highest energy are radiated, show the typical type 1 profiles of Hα light curves. On the contrary, in the light curve for $1.5 < I/I_0 < 2.5$, the second gradual maximum is outstandingly marked almost simultaneously with the soft X-ray maximum at about 06:33 UT. Since there is no outstandingly bright Hα-emitting region around this phase of the flare, the second gradual maximum must correspond to the maximum area of the Hα emitting region. Conventional Hα flare patrol films have never disclosed the first impulsive component of Hα emissions because of their low resolution and the saturation effect of photographic film, and their light curves have tended to reflect the time variation of the area of Hα emitting region. This probably led the existing textbooks by Švestka (1976) and Priest (1981) and others to miss the impulsive component of Hα emission.

5. Summary and Conclusion

The great two-ribbon flare of 12 October, 1981 was fully recorded with the Domeless Solar Telescope at the Hida Observatory. One hundred and forty seven pictures of Hα – 1.0 Å covering the impulsive phase through the post maximum phase of the flare were measured by the two-dimensional microdensitometers and extensively studied. This may be the first attempt to study the light curves of all bright points in a two-ribbon flare with high temporal and spatial resolution pictures.

The important findings of this work are:

(1) Hα light curves are classified into three typical shapes. The type 1 light curve is

characterized by an abrupt increase and rapid fall of intensity as seen in an impulsive spike of hard X-ray or microwave emissions. The type 2 shows a predominant gradual maximum which is attained in 2–3 min, though it often has one or two smaller impulsive peaks on its rising slope. The light curve of the type 3 is very different from the other two types and is characterized by much slower increase of intensity than the gradual rise of the type 2. The impulsive peaks of the type 1 and type 2 may be excited by energetic particle beams. The second gradual maximum of the type 1 and the main gradual maximum of the type 2 are assumed to be formed by the heat conduction front. The type 3 emission is excited by much slower heating agents, possibly by slower heat conduction or soft X-ray radiation. It is also possible that the very slow rise of the type 3 corresponds to the slow energy release in the high flare-loops at the late stage of the flare. The shapes of Hα light curves, therefore, provide us with a useful tool for examining the energy release and transport mechanisms in the flare loops of different locations of different types of flares.

(2) We first demonstrated the good temporal correlation between hard X-ray and Hα total intensity integrated over the whole Hα flare region, though the good correspondances between the successive brightenings of individual flare points or kernels and impulsive spikes of hard X-ray emissions have already been shown in our previous works (Kurokawa *et al.*, 1986; Kurokawa, 1986, Kurokawa, Takakura, and Ohki, 1988).

The traditional text books by Švestka (1976), Priest (1981), and others have failed to disclose correctly such an impulsive component of Hα emission closely correlated to the hard X-ray or microwave spikes, because their Hα light curves were derived from the conventional Hα flare patrol films of low resolution.

The studies of the spatial and temporal variations of Hα light curves and their correlations to X-ray and microwave emissions provide us with an important clue with which we can examine the energy release and transport mechanisms of flares. More observations with high spatial and temporal resolutions are necessary in future for different types of Hα flares together with X-ray and ratio observations.

References

Brown, J. C.: 1973, *Solar Phys.* **28**, 151.

Brown, J. C.: 1986, in D. F. Neidig (ed.), *The Lower Atmosphere of Solar Flares*, National Solar Observatory (Sacraments Peak Obs.)/Solar Maximum Mission Symposium, p. 431.

Kahler, S., Spicer, D., Uchida, Y., and Zirin, H.: 1980, in P. A. Sturrock (ed.), *Solar Flares*, Colorado Associated University Press, Boulder, Colorado, p. 83.

Kawaguchi, I., Kurokawa, H., Funakoshi, Y., and Nakai, Y.: 1982, *Solar Phys.* **78**, 101.

Kurokawa, H.: 1986, in D. F. Neidig (ed.), *The Lower Atomosphere of Solar Flares*, National Solar Observatory (Sacraments Peak Obs.)/Solar Maximum Mission Symposium, p. 51.

Kurokawa, H., Takakura, T., and Ohki, K.: 1988, *Publ. Astron. Soc. Japan* **40**, 357.

Kurokawa, H., Kitahara, T., Nakai, Y., Funakoshi, Y., and Ichimoto, K.: 1986, *Astrophys. Space Sci.* **118**, 149.

Priest, E. R. (ed.): 1981, *Solar Flare Magnetohydrodynamics*, Gordon and Breach, New York.

Švestka, Z.: 1976, *Solar Flares*, D. Reidel Publ. Co., Dordrecht, Holland.

Vorpahl, J. A.: 1972, *Solar Phys.* **26**, 397.